

# Possible chromosomal and germline integration of human herpesvirus 7

Bhupesh K. Prusty,<sup>1,\*</sup> Nitish Gulve,<sup>1</sup> Santa Rasa,<sup>2</sup> Modra Murovska,<sup>2</sup> Pilar Collado Hernandez<sup>3</sup> and Dharam V. Ablashi<sup>4</sup>

## Abstract

Human herpesvirus 7 (HHV-7) is a betaherpesvirus, and is phylogenetically related to both HHV-6A and HHV-6B. The presence of telomeric repeat sequences at both ends of its genome should make it equally likely to integrate into the human telomere as HHV-6. However, numerous studies have failed to detect germline integration of HHV-7, suggesting an important difference between the HHV-6A/-6B and HHV-7 genomes. In search of possible germline integrated HHV-7, we developed a sensitive and quantitative real-time PCR assay and discovered that primers designed against some parts of the HHV-7 genome can frequently miss HHV-7 positive clinical samples even though they work efficiently in cell-culture-derived HHV-7 positive materials. Using a primer pair against the U90 ORF of HHV-7, we identified a possible case of germline integration of HHV-7 with one copy of viral genome per cell in both peripheral blood cells and hair follicles. Chromosomal integration of HHV-7 in these individuals was confirmed by fluorescence *in situ* hybridization analysis. Germline integration of HHV-7 was further confirmed by detection of ~2.6 copies of HHV-7 in the hair follicles of one of the parents. Our results shed light on the complex nature of the HHV-7 genome in human-derived materials in comparison to cell-culture-derived materials and show the need for stringent criteria in the selection of primers for epidemiological HHV-7 studies.

## INTRODUCTION

*Human herpesvirus 7* (HHV-7) is a member of the genus *Roseolovirus* of the subfamily *Betaherpesvirinae*, and is closely related to HHV-6A and HHV-6B. It is lymphotropic, neurotropic, and shares disease associations such as febrile seizures, febrile status epilepticus, encephalitis and skin rash [1–6]. Like HHV-6B, HHV-7 is highly prevalent, with 75–90% of healthy adults harbouring the virus [7, 8]. Infectious HHV-7 is frequently present in the saliva of healthy humans [9]. However, unlike HHV-6A/-6B, little is known about the mechanisms of HHV-7 persistence and latency.

Although somewhat shorter (145 kb vs ~160 kb) and overall more compactly arranged, the HHV-7 genome shares similarities with both HHV-6A and HHV-6B genomes, including eukaryotic-telomere-related sequence arrays in the direct repeat (DR) elements at the ends of the respective genomes (DR<sub>L</sub> and DR<sub>R</sub>) [1]. The presence of telomeric repeats at HHV-6A/-6B genomic termini enables the viral genomes to

integrate into host-cell telomeres via homologous recombination [10, 11]. Such integration can occur in germline cells to initiate genetic lineages in which the virus genome is transmitted to offspring through the germline, resulting in genomic integration of the virus in a specific chromosome in every nucleated cell [12–14]. This germ-line chromosomally integrated HHV-6 (ciHHV-6) can be activated to a transmissible infectious form in cultured cells [15–18]. Recent evidence suggests that the integrated virus can produce infectious virions *in vivo* in pregnant ciHHV-6 women [13] and under conditions of immunosuppression [19]. Excision of chromosomally integrated viral genomes appears to occur via homologous-recombination-mediated telomeric circle (t-circle) formation [16, 17].

Based on the similarities between HHV-6A, HHV-6B and HHV-7, we hypothesized that HHV-7 genomes might also integrate into human telomeres in a manner similar to HHV-6. While developing a sensitive and quantitative PCR assay, we observed that certain genomic regions of HHV-7, in *in vivo* patient samples as well as *in vitro* cultured cells

Received 6 December 2016; Accepted 19 December 2016

**Author affiliations:** <sup>1</sup>Department of Microbiology, Biocenter, University of Würzburg, 97074 Würzburg, Germany; <sup>2</sup>August Kirchenstein Institute of Microbiology and Virology, Riga Stradins University, 1069 Riga, Latvia; <sup>3</sup>Hospital Clinico Universitario Lozano Blesa, 50009 Zaragoza, Spain; <sup>4</sup>HHV-6 Foundation, Santa Barbara, CA 93101, USA.

**\*Correspondence:** Bhupesh K. Prusty, bhupesh.prusty@biozentrum.uni-wuerzburg.de

**Keywords:** HHV-7; HHV-6; ciHHV-6; chromosomal integration.

**Abbreviations:** ciHHV-6, chromosomally integrated human herpesvirus 6; C<sub>q</sub>, quantification cycle; DR, direct repeat; FISH, fluorescence *in situ* hybridization; HHV, human herpesvirus; LOD, limit of detection; qPCR, quantitative real-time PCR; RT-PCR, reverse-transcription PCR; wpi, weeks post-infection.

Two supplementary tables are available with the online Supplementary Material.

carrying integrated HHV-7, are easily amplifiable by PCR whereas others are not. Genetic polymorphism between HHV-7 in the human population has been described elsewhere [20]. However, we could not see sequence variations that could explain the differences in the PCR results between HHV-7 positive *in vivo* patient materials and *in vitro* cell-culture-derived samples. However, using a newly developed primer pair against the HHV-7 U90 ORF, we were able to detect HHV-7 in all patient samples, which helped us identify two possible cases of germline integration of HHV-7 genomes.

## RESULTS

### Development of quantitative real-time PCR (qPCR) assays and a cell line carrying latent chromosomally integrated HHV-7

We compared the genome sequences of HHV-7 type JI (U43400.1), RK (AF037218.1) and UCL-1 (KF558370.1) strains, and selected four different regions of the HHV-7 genome [U4, U54, gB (glycoprotein B) and U90] that had 100 % conserved sequences among these strains. In order to develop a standard curve, we amplified stretches of HHV-7 DNA from these four regions of HHV-7(JI) strain undergoing active infection in SupT1 cells (Fig. 1a) using viral-gene-specific primers [indicated as external primers to mark them different from another internal set of primers within the same region (Table S1, available in the online Supplementary Material)] and cloned them into pCR2.1 vector to create a known number of copies of the desired viral genomic region. Using a second set of internal primers (Table S1) and 10-fold serial dilutions of a known number of viral genomic copies, we tested and created standard curves that showed amplification of 10 to 10<sup>6</sup> genome equivalents of the desired viral DNA with more than 99 % efficiency (Fig. 1b) [limit of detection (LOD) = 10 copies per reaction] in the presence of spiked cellular DNA. Total cellular DNA (100 ng) containing a known number of genome equivalents of viral DNA was used in every qPCR reaction. We amplified the cellular gene PI15, present at two copies per human cell, in parallel [18] to normalize the viral genome copy number and to calculate the number of host cell copies per reaction. HHV-7(JI)-infected SupT1 cultured cells were used as a positive control because amplicons were successfully obtained using total DNA derived from these cells in all the four primer pairs.

To test the efficiency of these primers in the case of latent virus infection, we created a latent HHV-7-like cell line by infecting SupT1 cells with HHV-7(RK) strain (named hereafter as Sup.H7). After long-term passaging and cell sorting, we identified a single-cell-derived clone that continuously remained HHV-7 positive (Fig. 2a, Table 1) without any visual signs of productive viral infection (no cytopathic effect). These cells were treated with a known inducer of ciHHV-6, hydrocortisone (10<sup>-5</sup> M) [15, 18] to activate viral DNA replication. Enlargement of the cell body, a hallmark of HHV-7 activation, was found in 5–10 % of the infected

cells within 2 weeks of hydrocortisone treatment (Fig. 2b). The amount of viral DNA was quantified by qPCR using the internal U4 primer pair, which showed increased viral load. Hydrocortisone treatment increased the viral load up to 12-fold by 5 weeks post-infection (wpi) (Fig. 2c). Immunostaining of activated cells using two different mAbs against HHV-7 early antigen U27 and late antigen (KR4), which detects an unknown late viral protein [21, 22], was positive, confirming the reactivation of HHV-7 (Fig. 2d). U27 was detected mostly within the nucleus of activated cells, whereas KR4 antibody detected viral proteins within the cytoplasm of activated cells. To assess viral genes associated with activation, viral transcription was analysed in the activated cells in comparison to the untreated counterpart cells using different primer pairs. Interestingly, we observed transcription of HHV-7 U4 and gB (Fig. 2e) only in hydrocortisone-treated cells at 2 wpi, indicating that these transcripts might serve as a marker for viral activation. HHV-7 U90, U20 and U54 transcripts were detected in lower amounts in non-activated cells, which subsequently increased after viral reactivation.

Transmission electron microscopy confirmed herpesvirus-like particles that lacked discernible envelopes (Fig. 2f), thereby indicating incomplete viral activation. Consistent with this, very little infectivity was recovered. These Sup.H7 cells carrying quiescent HHV-7(RK) were tested for chromosomal integration by fluorescence *in situ* hybridization (FISH) analysis (Fig. 2g), which showed probable telomeric integration of HHV-7. With these results, we confirmed generation of a clonal population of cells with chromosomally integrated HHV-7, which was in a latent stage and capable of reactivation with external stimuli.

Total cellular DNA from these cells was tested using all four internal qPCR primer pairs, which detected ~1 genome equivalent of HHV-7 per cell (Tables 1 and S2). DNA from these cells was used as a positive control in all the subsequent qPCR studies. With this we validated a latent HHV-7 cell line that carried ~1 copy of HHV-7 in a chromosomally integrated state and four pairs of primers that amplified four different viral regions with equal efficiency.

### Possible germline integration of HHV-7 in two individuals

As a next step, we tested the effectiveness of our qPCR assays to detect HHV-7 in additional patient-derived DNA samples. In the course of the investigation, we came across two unusual clinical cases positive for HHV-7. In the first case (patient 1), a 1-day-old newborn was detected with hypoglycaemia. During routine testing carried out in such cases, HHV-7 was detected by PCR in cerebrospinal fluid, but not in serum. The baby tested negative for HHV-6, Epstein-Barr virus, human cytomegalovirus and other pathogens in the cerebrospinal fluid. Serum samples from the mother and the father were also negative for HHV-7. We analysed DNA derived from the whole blood of this child as well as hair follicles for HHV-7 (Table 1). We detected a low level of HHV-7 in the whole blood (0.01 genome equivalents per cell), but 1 genome

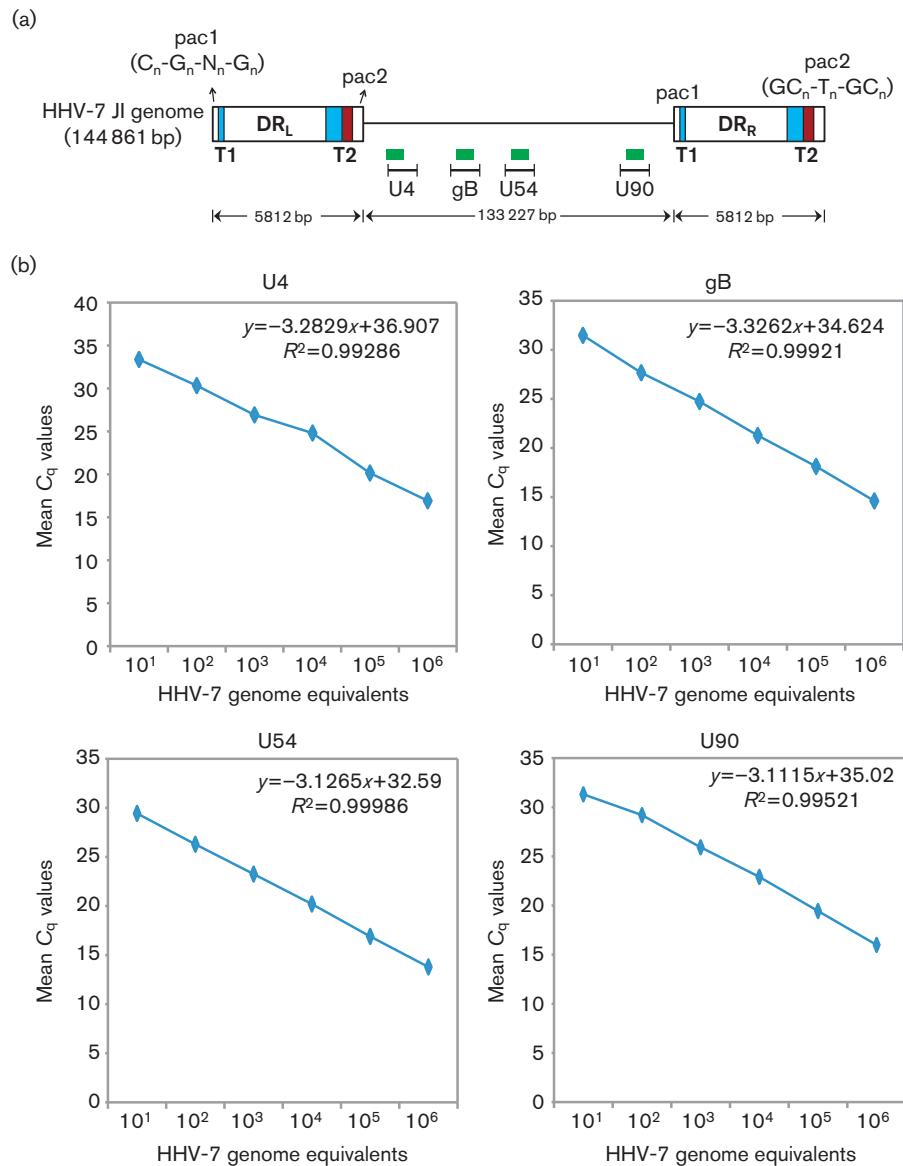


**Fig. 1.** qPCR assay to detect HHV-7. (a) Schematic representation showing approximate location of the four different regions of the HHV-7 genome selected for PCR analysis. Similarities between the genomic organization of HHV-6A (HHV-6B) and HHV-7 are marked by DR<sub>L</sub> and DR<sub>R</sub>; packaging signal sequences (pac1 and pac2) within the HHV-7(JI) (GenBank accession no. U43400.1) are shown. Stretches of heterogeneous telomeric repeat sequences are indicated by blue boxes, and stretches of homogeneous telomeric repeat sequences are indicated by red boxes. DR<sub>L</sub>, Left DR; DR<sub>R</sub>, right DR; T1, telomeric repeat 1; T2, telomeric repeat 2. (b) Standard curve analysis of U4, U54, gB and U90 regions of HHV-7 using specific primer pairs. Tenfold serial dilutions of plasmids carrying the respective regions were tested in triplicate by qPCR. Mean quantification cycle (C<sub>q</sub>) values are plotted against the copy numbers. Correlation coefficients and slope values are given in each graph panel.

equivalent of HHV-7 per cell in hair follicles (Table 1) using the U90 primer pair, whereas other primer pairs could not amplify viral DNA in both types of samples. Similar results were also obtained from whole-blood and hair-follicle samples derived from the mother (0.01 genome equivalents of HHV-7 per cell in whole blood but 1 genome equivalent per cell in the hair follicles) (Table 1). We could not obtain samples from the father. Genetic polymorphism and sequence variations of

HHV-7 in the human population have been described in the past [20] that can prevent PCR amplification. Hence, we used three of the external primer pairs (U54, gB and U90) to amplify HHV-7 genomic regions from blood and hair follicles in both the mother and the baby, and detected a very low amount of PCR DNA in some of the samples (Fig. 3a). Purified PCR products were sequenced directly and were compared to those obtained from Sup.H7 cells having the HHV-7

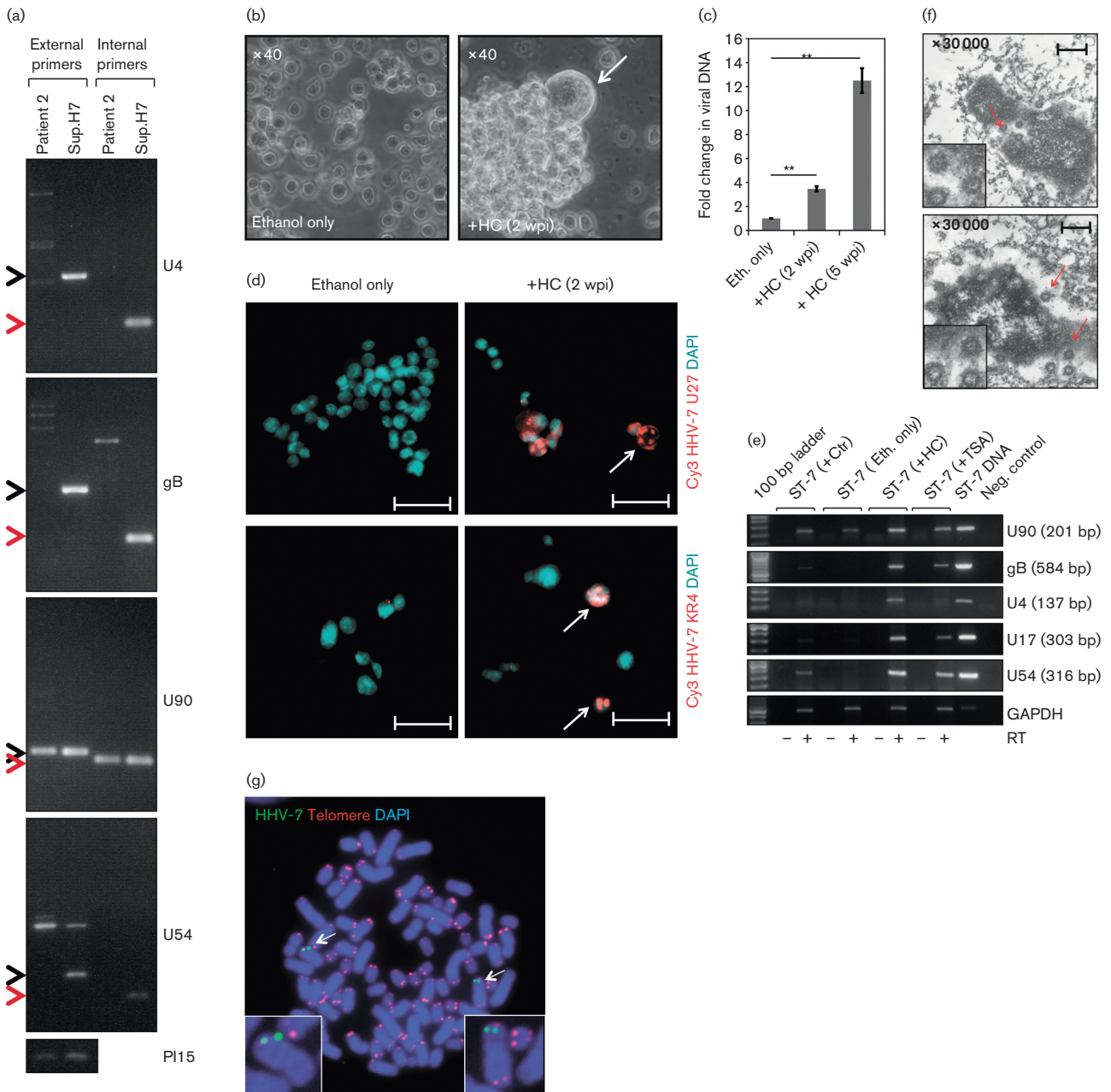


**Fig. 2.** Sup.H7 cells carry ~1 genome equivalent of latent and chromosomally integrated HHV-7. (a) The PCR efficiency of four sets of primers was tested in Sup.H7 cells and compared to that of blood-derived DNA from patient 2. Amplimers from external primer pairs are marked by black arrowheads and those from internal primer pairs are marked by red arrowheads. (b) Activated Sup.H7 cells induce syncytia formation. Sup.H7 cells were treated with  $10^{-5}$  M hydrocortisone for 2 weeks. Enlarged cells (marked with a white arrow) representing activated HHV-7 were detected forming large clumps (right panel) by phase contrast microscopy. Solvent control (ethanol) treated cells (left panel) did not show such characteristic features of viral activation. (c) The increase in the amount of viral DNA was quantified by qPCR. Sup.H7 cells were treated with  $10^{-5}$  M hydrocortisone for different time intervals. Total genomic DNA was isolated and used for qPCR. Ethanol-treated (Eth. only) cells were used as a control. \*\*,  $p < 0.005$ . (d) Immunostaining using mAbs against HHV-7 (red staining in the images) identified activated Sup.H7 cells. Hydrocortisone treatment was carried out for 2 wpi. HHV-7-specific staining is marked with white arrows. DAPI staining is blue/green in the images. Bars, 50  $\mu$ m. (e) Transcription profile of viral genes after HHV-7 activation in Sup.H7 cells. Total RNA from Sup.H7 cells, either infected with *Chlamydia trachomatis* (+Ctr) for 2 weeks or treated with different chemical stimuli like trichostatin A (TSA) or hydrocortisone, was used for reverse transcription PCR (RT-PCR). Primers designed against HHV-7 U4, U20, U54, U90 and gB were used for the the PCR. Amplification of GAPDH was used as a control. (f) Transmission electron microscopy identified unique herpesvirus-like particles after hydrocortisone treatment in induced cells. The insets show a few viral particles at higher magnification identifying nucleoid, nuclear membrane and tegument, yet no envelope. These viral structures are comparable with HHV-7 particles. Both pictures (top and bottom panels) represent hydrocortisone-

treated activated Sup.H7 cells from two independent experiments. Bars, 0.5  $\mu$ m. Red arrows indicate viral particle like structures. (g) FISH image of Sup.H7 cells showing the association of HHV-7 with host cell chromosomes. Sup.H7 metaphase spreads were stained with a Cy5-labelled HHV-7 probe (green) and a FITC-labelled telomeric PNA probe (red). DNA was stained with DAPI (blue). Chromosomal integration sites of HHV-7 are indicated with white arrows at 60 $\times$  magnification. Due to the tetraploid nature of the cells, two integration sites are detected within a single metaphase spread. The insets show magnified images of chromosomes carrying integrated HHV-7. HC, Hydrocortisone

(RK) strain. We could not see any sequence variations within the analysed genomic regions. Subsequent FISH analysis using peripheral-blood-derived PBMCs from both the baby (Fig. 3b) and the mother (Fig. 3c) detected integrated HHV-7 in the telomeric regions of a few cells supporting possible rare chromosomal integration of HHV-7.

In a second case (patient 2), a 34-year-old male suffering from chronic fatigue syndrome tested positive for HHV-7 during routine analysis using a commercial kit (Genesig; PrimerDesign). We tested the blood-derived DNA from this patient in our qPCR assay and found 1 genome equivalent of HHV-7 per cell in the blood (Table 1). Like our previous results, only the U90 primer pair successfully amplified the viral genome, whereas U4, U54 and gB primer pairs could not detect any viral DNA (Fig. 2a). Subsequently, we tested hair follicles from this patient and found  $\sim$ 1 genome equivalent of HHV-7 per cell using only the U90 primer pair (Table 1). Analysis of hair follicles from both the parents detected  $\sim$ 2.6 genome equivalents of HHV-7 per cell in the mother's hair, whereas no viral DNA was detected in the father (Table 1). We could not get consent from both the parents for blood collection and analysis. Subsequent FISH analysis using blood-derived PBMCs from the patient detected possible integrated

HHV-7 in the telomeric regions (Fig. 3d). Thus, we found strong evidence for possible chromosomal integration and genetic inheritance of HHV-7.

We utilized DNA derived from the blood of patient 2 having 1 copy of HHV-7 per cell in blood and hair follicles for further analysis of negative PCR results from certain viral genomic regions. The presence of complex and highly stable genomic structures, including but not limited to hairpin stem-loop structures and G-quadruplexes [23], within the target region might inhibit the efficiency of PCR amplifications. To verify such a situation leading to inefficient PCR amplification within U4, gB and U54, we carried out nested PCRs using the internal primers and the PCR amplimers derived using external primer pairs (Fig. 3e). The desired PCR products were obtained during the nested PCR of gB and U54 regions, suggesting that due to some unknown factors PCR amplification from U54 and gB was not highly effective during the first PCR. Nested PCR products were further sequenced to validate the amplimers. These results suggested that even if most of the viral genomes are present within a sample, successful identification and quantification of the HHV-7 might depend upon the sample type and the efficiency of the selected primers to amplify that genomic region.

**Table 1.** HHV-7 copy numbers as quantified by qPCR in different types of biological materials

Sample	U4		U54		gB		U90		PI15		HHV-7 U90 copies per cell
	C <sub>q</sub>	Calculated copies	C <sub>q</sub>	Calculated copies	C <sub>q</sub>	Calculated copies	C <sub>q</sub>	Calculated copies	C <sub>q</sub>	Calculated cell numbers	
<b>Sup.H7 (positive control)</b>											
Cultured-cell-derived DNA (Sup.H7)	26.34	1655	22.5	1687.5	23.9	1639.6	25	1660.7	22.26	1639.11	$\sim$ 1.1
<b>Case 1</b>											
Blood (patient 1)	34.13	7.01*	35.12	0.155*	32.56	3.88*	30.04	39.76	21.27	3673.88	0.01
Hair (patient 1)	37.15	0.84*	36.79	0.04*	33.15	2.57*	28.91	91.54	26.00	77.7	1.17
Blood (mother of patient 1)	35.02	3.75*	34.97	0.17*	32.97	2.91*	28.51	123.571	19.89	11314	0.01
Hair (mother of patient 1)	34.92	4.02*	37.12	0.03*	31.68	7.18*	29.79	47.95	26.69	44.27	1.07
<b>Case 2</b>											
Blood (patient 2)	33.87	8.41*	27.05	59.09	32.12	5.28*	20.34	52056.04	18.17	45658	1.14
Hair (patient 2)	34.32	6.13*	34.30	0.28*	31.45	8.43*	29.15	76.56	26.23	64.4	1.18
Hair (mother of patient 2)	36.12	1.73*	37.45	0.02*	32.33	4.56*	29.5	59.21	27.49	23.06	2.6
Hair (father of patient 2)	37.38	0.71*	34.97	0.02*	32.13	5.24*	32.98	4.52*	27.86	34.11	<LOD

\*Below LOD.

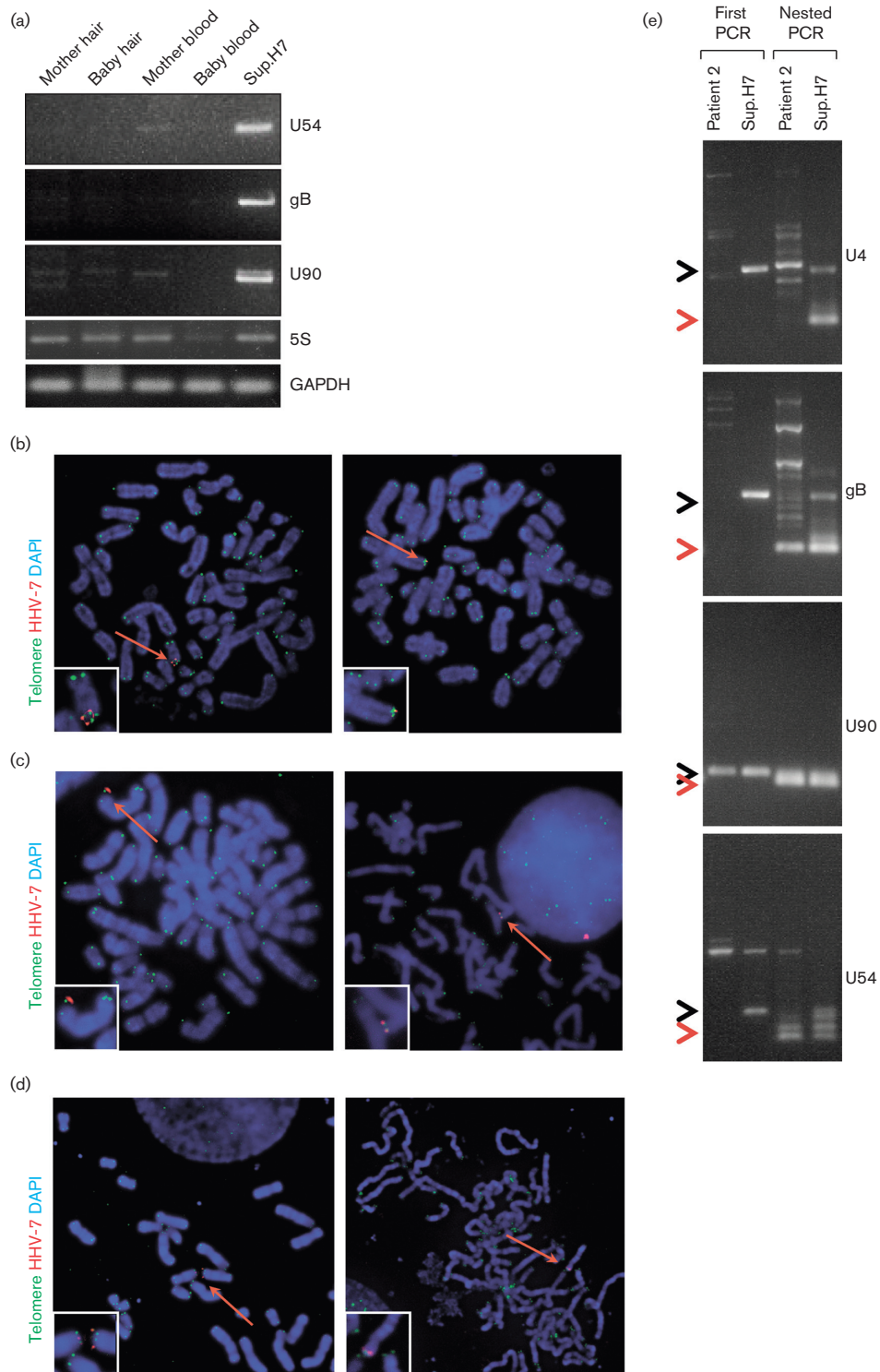


**Fig. 3.** Chromosomal integration and possible inheritance of HHV-7. (a) HHV-7 U54, gB and U90 were amplified from the blood- and hair-follicle-derived DNA of patient 1 and his mother using external pairs of primers. DNA from Sup.H7 cells was used as a positive control. GAPDH and 5S were amplified to check the DNA quality in all the samples. (b) Chromosomal integration of HHV-7 in the peripheral blood cells of patient 1 was tested by FISH analysis. IL2-stimulated PBMCs from patient 1 were used for metaphase-spread preparation and were co-stained with a Cy5-labelled HHV-7 probe (red) together with a FITC-labelled telomeric PNA probe (green). DNA was stained with DAPI (blue). Chromosomal integration sites of HHV-7 are indicated with arrows at 60× magnification. Magnified images of chromosomes carrying integrated HHV-7 are highlighted in the insets. Images from two independent experiments are shown. (c) Chromosomal integration of HHV-7 in the peripheral blood cells of the mother of patient 1 was tested by FISH analysis as

above. (d) Chromosomal integration of HHV-7 in the peripheral blood cells of patient 2 was tested by FISH analysis as above. (e) The PCR efficiency of the four sets of primers was tested in Sup.H7 cells and compared to that of nested PCR using blood-derived DNA from patient 2. Amplimers from external primer pairs are marked by black arrowheads and those from nested PCR with internal primer pairs are marked by red arrowheads.

## DISCUSSION

The presence of similar telomeric repeat sequences at the genomic ends of both HHV-6 and HHV-7 suggests the possibility of telomeric integration and germline inheritance of all the three betaherpesviruses. However, there is no documented evidence for chromosomal integration of HHV-7. Moreover, it is believed that HHV-7 is not transmitted vertically via germline integration, as is the case with *ici*HHV-6A and -6B, as no congenital HHV-7 was detected in a large study based on 2129 cord-blood samples [24]. Given the fact that there have been occasional reports of cases with very high levels of HHV-7, the possibility of germ-line transmitted HHV-7 should be explored. With an aim to compare the amplification efficiency of various primer pairs designed against different HHV-7 ORFs, we designed a real-time PCR-based quantitative assay with a LOD of up to 10 genome equivalents of HHV-7 genome with more than 99 % efficiency within a complex mixture of human genomic DNA. These primer pairs were further validated in newly developed Sup.H7 cells carrying latent and chromosomally integrated HHV-7 infection. During further experimental validation of the primer pairs, we faced an unprecedented situation, in which three of the primer pairs (U4, gB and U54) were unable to amplify viral genome in human-patient-derived genomic DNA containing HHV-7. In one of the cases (patient 1), we used external primer pairs and were able to amplify low levels of HHV-7. After sequence analysis of these amplimers, we could not detect any alterations within the genomic regions that could prevent primer binding. The low levels of viral DNA amplified by U4, gB and U54 primers (Fig. 3a) could originate from superinfected viral DNA, preventing any conclusion being made regarding the origin of the viral DNA. However, our study strongly suggests that primer design can play a crucial role in HHV-7 detection. Primers designed against U90 were highly efficient in cell-culture-derived materials as well as human biological samples, whereas primers against U4, gB and U54 were not efficient against viral DNA derived from *in vivo* patient materials.

G-rich DNA within eukaryotic genomes can form highly stable G-quadruplex tetrad structures, which are known to inhibit sequence-specific amplification of DNA [23, 25]. Bioinformatic sequence analysis using QGRS Mapper [26] predicted the possible formation of G-quadruplex structures within the reverse primer binding regions of one of the primer pairs (gB). This might explain the complex nature of the sequences within this region that could prevent reverse primer binding in human clinical samples. However, we did not detect a stable genomic structure within the U4 and U54 region that could also prevent primer binding.

Moreover, it is difficult to understand the sequence complexity of the same viral DNA under natural infection conditions and *in vitro* cell culture that decides DNA synthesis capability. Our results clearly show that primers designed and validated with cell culture infected virus may not work with equal efficiency in clinical materials. Extreme caution should be taken while designing primers for PCR-based epidemiological studies and primers should be extensively validated using positive clinical materials.

We analysed the possibility of chromosomal integration of HHV-7 in various cell types including cells from HHV-7 positive patients and found evidence for chromosomal integration of HHV-7 into host cell telomeres suggesting HHV-7 to be the third roseolovirus known to integrate into human telomeric repeat sequences. We identified two clinical cases carrying latent HHV-7 in hair follicles. However, we detected 1 genome equivalent of HHV-7 in the blood of one of the cases (patient 2) and ~2.6 viral genome equivalents in the hair follicle of his mother, suggesting a possible case of inheritance of chromosomally integrated latent HHV-7. However, we could not find similar copies of latent viral genome in the blood of patient 1 and his mother. We could only detect 0.01 genome equivalents of viral DNA per cell by qPCR and integrated viral DNA in a few blood cells by FISH. This might suggest the highly unstable nature of integrated viral DNA in fast-replicating cells. However, HHV-7 shares CD4<sup>+</sup> T-cell specificity [27] with varicella zoster virus [28], suggesting the possibility of similar infection properties to varicella zoster virus, which accumulates in the skin at the base of hair follicles [29, 30] after initial replication. Thus, endothelial cells at the base of hair follicles could provide a unique niche for the virus to achieve latency.

Here, we report the generation of a latent HHV-7 cell line (Sup.H7) carrying ~1 genome equivalent of HHV-7 per cell that could be reactivated using chemical stimuli like trichostatin A and hydrocortisone. Our study provides the first-ever molecular evidence, to our knowledge, for possible chromosomal integration of HHV-7, and demonstrates activation of latent chromosomally integrated HHV-7 under the influence of chemical stimuli. HHV-7 has been associated with seizures and encephalitis, and reactivates rarely in transplant patients' skin diseases. New insight into HHV-7 latency and its activation should encourage researchers to expand investigations into the possible role of the virus in human disorders.

## METHODS

All the methods were carried out in accordance with approved guidelines.

## Cell lines and HHV-7 infection

Sup.H7 and SupT1 cells were grown in RPMI 1640 media containing 5–10 % FBS at 37 °C and 5 % CO<sub>2</sub>. Productive infection of SupT1 cells with HHV-7(JI) has been described elsewhere [31].

## Generation of Sup.H7 cells

The Sup.H7 cell line was generated by co-cultivating uninfected SupT1 cells [31] with HHV-7(RK)-infected cells at a ratio of 9:1 and then culturing the cells for 2–3 months until the cells lost all signs (ballooning, refractile cytopathic effect, no expression of late viral proteins) of active viral infection but still contained a mean of >1 virus genome per cell. The presence of HHV-7 genomes in the Sup.H7 cells was confirmed by fluorescence *in situ* hybridization. Viral latency in these cells was confirmed by analysing viral copy number in the absence of a detectable amount of late viral mRNAs or viral glycoproteins.

## Preparation of plasmids and standard curve analysis

To generate known numbers of copies of viral genome for standard curve analysis, HHV-7 genomic regions were amplified and purified PCR products were cloned into TOPO pCR 2.1 vector (Life Technologies). Cloned DNA vectors were used to transform *Escherichia coli* DH5 $\alpha$  and propagated to isolate ample amount of vectors for qPCR analysis. Cloned ORFs were verified by DNA sequencing. Standard curve analysis for human PI15 ORF has been described before [18].

## Primers and probes

A cocktail mixture of five different purified PCR products amplified from different genomic regions of HHV-7(JI) was used as a FISH probe. The sequences of oligomers used to amplify probe sequences by PCR are provided in Table S1. After purification, the amplimers were labelled with the Cy5 fluorophore using a nick translation kit (PromoFluor-640 nick translation labelling kit; PromoKine) and then purified before use. FITC-labelled C-rich telomere probe (PN-TC011-005) was purchased from Eurogentech.

## *Chlamydia trachomatis* infection

Sup.H7 cells were infected with *C. trachomatis* strain LGV-L2 434/Bu at an m.o.i. of 1–5 as described previously [16, 18].

## DNA extraction

Genomic DNA from the peripheral blood of patient 1 and patient 2 and cultured cells was extracted using a QIAamp DNA mini kit (Qiagen) following the manufacturer's protocol. DNA extraction from hair follicles was carried out using QuickExtract DNA extraction solution (Epicentre) and Extracta DNA Prep PCR – tissue (Quanta Biosciences).

## qPCR

qPCR was carried out and is explained here following the published MIQE guidelines [32]. PerfeCTa qPCR SuperMix (Quanta Biosciences) was used for qPCR. Amplifications

were done on a StepOnePlus real-time PCR platform (Applied Biosciences) using the manufacturer's protocol and SYBR Green chemistry. Amplification data were analysed using StepOne software v2.1. A total of 100–150 ng cellular DNA was used for every reaction. Total DNA isolated from SupT1 cells carrying active HHV-7(JI) infection and Sup.H7 cells carrying latent HHV-7 genome were used as positive controls in every reaction. Amplification of cellular gene PI15 was used for normalization and calculation of the number of cell copies in every reaction.

## Nested PCR

For nested PCR, the first PCR amplification was carried out only for 25 cycles. The PCR product obtained was diluted 100 times and was used for nested PCR for another 25 cycles. All the semi-quantitative PCRs were carried out using the following temperature profile: initial denaturation at 98 °C for 2 min; 25 cycles of denaturation at 95 °C for 30 s, primer binding at 60 °C for 30 s and primer extension at 72 °C for 30 s; final extension at 72 °C for 20 min.

## Immunofluorescence microscopy

Cells were washed in PBS and fixed with 4 % paraformaldehyde for 30 min at room temperature. After washing, cells were permeabilized using 0.2 % Triton X-100 in PBS for 15 min and blocked with 10 % FCS in PBS for 1 h at room temperature. Cells were incubated for 1 h with the primary antibody in blocking buffer (2 % FCS in PBS), washed three times in PBS and stained with the corresponding secondary antibody. DAPI was used for staining cell nuclei. After washing three times with PBS, samples were mounted onto slides using Mowiol (Carl Roth). Samples were analysed with a Leica DMR epifluorescence microscope. HHV-7 U27 and KR4 antibodies were obtained from the HHV-6 Foundation, USA.

## RNA extraction and semi-quantitative reverse-transcription PCR (RT-PCR)

RNA extraction, cDNA synthesis and subsequent semi-quantitative RT-PCR were performed as previously described [33].

## Funding information

This work was supported by a grant from the VolkswagenStiftung (grant no. 88773) to B.K.P. under the Volkswagen Foundation's funding initiative 'Experiment!'. M.M. and S.R. were supported by project BALTINFECT (no. 316275) within the European Union 7th Framework Programme (no. RSU ZP 13/2013) and a grant from the Latvian Council of Sciences (no. 478/2012).

## Acknowledgements

We thank Professor Thomas Rudel for supporting our work at the Department of Microbiology, University of Würzburg. We thank the HHV-6 Foundation, USA, for providing antibodies for this study. We specially thank Kristin Loomis from the HHV-6 Foundation for her excellent support during the study design process, her comments/suggestions throughout the study and her critical evaluation of the manuscript. We thank Professor Georg Krohne, University of Würzburg, for the electron microscopy core facility, and Professor Carol Burke and Professor Gerhard R. F. Krueger for their expert advice on electron microscopy images.



**Conflicts of interest**

The authors declare that there are no conflicts of interest.

**Ethical statement**

Patient 2 was recruited in Latvia with informed consent and with the approval of the Ethics Committee of the Riga Stradins University. Blood and hair follicles from patient 1 were collected at the Paediatrics Department, Hospital Clinico Universitario Lozano Blesa, Spain, with written consent.

**References**

- Krug LT, Pellett PE. Roseolovirus molecular biology: recent advances. *Curr Opin Virol* 2014;9:170–177.
- Black JB, Pellett PE. Human herpesvirus 7. *Rev Med Virol* 1999;9:245–262.
- Frenkel N, Schirmer EC, Wyatt LS, Katsafanas G, Roffman E et al. Isolation of a new herpesvirus from human CD4+ T cells. *Proc Natl Acad Sci USA* 1990;87:748–752.
- Yoshikawa T, Ihira M, Suzuki K, Suga S, Matsubara T et al. Invasion by human herpesvirus 6 and human herpesvirus 7 of the central nervous system in patients with neurological signs and symptoms. *Arch Dis Child* 2000;83:170–171.
- Torigoe S, Koide W, Yamada M, Miyashiro E, Tanaka-Taya K et al. Human herpesvirus 7 infection associated with central nervous system manifestations. *J Pediatr* 1996;129:301–305.
- Berneman ZN, Gallo RC, Ablashi DV, Frenkel N, Katsafanas G et al. Human herpesvirus 7 (HHV-7) strain J1: independent confirmation of HHV-7. *J Infect Dis* 1992;166:690–691.
- Krueger GR, Koch B, Leyssens N, Berneman Z, Rojo J et al. Comparison of seroprevalences of human herpesvirus-6 and -7 in healthy blood donors from nine countries. *Vox Sang* 1998;75:193–197.
- Kozireva S, Nemceva G, Danilane I, Pavlova O, Blomberg J et al. Prevalence of blood-borne viral infections (cytomegalovirus, human herpesvirus-6, human herpesvirus-7, human herpesvirus-8, human T-cell lymphotropic virus-I/II, human retrovirus-5) among blood donors in Latvia. *Ann Hematol* 2001;80:669–673.
- Black JB, Inoue N, Kite-Powell K, Zaki S, Pellett PE. Frequent isolation of human herpesvirus 7 from saliva. *Virus Res* 1993;29:91–98.
- Morissette G, Flamand L. Herpesviruses and chromosomal integration. *J Virol* 2010;84:12100–12109.
- Kaufner BB, Flamand L. Chromosomally integrated HHV-6: impact on virus, cell and organismal biology. *Curr Opin Virol* 2014;9:111–118.
- Gravel A, Sinnott D, Flamand L. Frequency of chromosomally-integrated human herpesvirus 6 in children with acute lymphoblastic leukemia. *PLoS One* 2013;8:e84322.
- Gravel A, Hall CB, Flamand L. Sequence analysis of transplacentally acquired human herpesvirus 6 DNA is consistent with transmission of a chromosomally integrated reactivated virus. *J Infect Dis* 2013;207:1585–1589.
- Daibata M, Taguchi T, Nemoto Y, Taguchi H, Miyoshi I. Inheritance of chromosomally integrated human herpesvirus 6 DNA. *Blood* 1999;94:1545–1549.
- Arbuckle JH, Medveczky MM, Luka J, Hadley SH, Luegmayr A et al. The latent human herpesvirus-6A genome specifically integrates in telomeres of human chromosomes in vivo and in vitro. *Proc Natl Acad Sci USA* 2010;107:5563–5568.
- Prusty BK, Krohne G, Rudel T. Reactivation of chromosomally integrated human herpesvirus-6 by telomeric circle formation. *PLoS Genet* 2013;9:e1004033.
- Huang Y, Hidalgo-Bravo A, Zhang E, Cotton VE, Mendez-Bermudez A et al. Human telomeres that carry an integrated copy of human herpesvirus 6 are often short and unstable, facilitating release of the viral genome from the chromosome. *Nucleic Acids Res* 2014;42:315–327.
- Prusty BK, Siegl C, Hauck P, Hain J, Korhonen SJ et al. *Chlamydia trachomatis* infection induces replication of latent HHV-6. *PLoS One* 2013;8:e61400.
- Endo A, Watanabe K, Ohye T, Suzuki K, Matsubara T et al. Molecular and virological evidence of viral activation from chromosomally integrated human herpesvirus 6A in a patient with X-linked severe combined immunodeficiency. *Clin Infect Dis* 2014;59:545–548.
- Franti M, Gessain A, Darlu P, Gautheret-Dejean A, Kosuge H et al. Genetic polymorphism of human herpesvirus-7 among human populations. *J Gen Virol* 2001;82:3045–3050.
- de Vries HJ, Teunissen MB, Zorgdrager F, Picavet D, Cornelissen M. Lichen planus remission is associated with a decrease of human herpes virus type 7 protein expression in plasmacytoid dendritic cells. *Arch Dermatol Res* 2007;299:213–219.
- Miyoshi H, Tanaka-Taya K, Hara J, Fujisaki H, Matsuda Y et al. Inverse relationship between human herpesvirus-6 and -7 detection after allogeneic and autologous stem cell transplantation. *Bone Marrow Transplant* 2001;27:1065–1070.
- Wang Q, Liu JQ, Chen Z, Zheng KW, Chen CY et al. G-quadruplex formation at the 3' end of telomere DNA inhibits its extension by telomerase, polymerase and unwinding by helicase. *Nucleic Acids Res* 2011;39:6229–6237.
- Hall CB, Caserta MT, Schnabel KC, Boettlich C, Mcdermott MP et al. Congenital infections with human herpesvirus 6 (HHV6) and human herpesvirus 7 (HHV7). *J Pediatr* 2004;145:472–477.
- Boán F, Blanco MG, Barros P, González AI, Gómez-Márquez J. Inhibition of DNA synthesis by K+-stabilised G-quadruplex promotes allelic preferential amplification. *FEBS Lett* 2004;571:112–118.
- Kikin O, D'Antonio L, Bagga PS. QGRS Mapper: a web-based server for predicting G-quadruplexes in nucleotide sequences. *Nucleic Acids Res* 2006;34:W676–W682.
- Lusso P, Secchiero P, Crowley RW, Garzino-Demo A, Berneman ZN et al. CD4 is a critical component of the receptor for human herpesvirus 7: interference with human immunodeficiency virus. *Proc Natl Acad Sci USA* 1994;91:3872–3876.
- Moffat JF, Stein MD, Kaneshima H, Arvin AM. Tropism of varicella-zoster virus for human CD4+ and CD8+ T lymphocytes and epidermal cells in SCID-hu mice. *J Virol* 1995;69:5236–5242.
- Zerboni L, Sen N, Oliver SL, Arvin AM. Molecular mechanisms of varicella zoster virus pathogenesis. *Nat Rev Microbiol* 2014;12:197–210.
- Ku CC, Zerboni L, Ito H, Graham BS, Wallace M et al. Varicella-zoster virus transfer to skin by T cells and modulation of viral replication by epidermal cell interferon-alpha. *J Exp Med* 2004;200:917–925.
- Ablashi DV, Handy M, Bernbaum J, Chatlynne LG, Lapps W et al. Propagation and characterization of human herpesvirus-7 (HHV-7) isolates in a continuous T-lymphoblastoid cell line (SupT1). *J Virol Methods* 1998;73:123–140.
- Bustin SA, Benes V, Garson JA, Hellemans J, Huggett J et al. The MIQE guidelines: minimum information for publication of quantitative real-time PCR experiments. *Clin Chem* 2009;55:611–622.
- Prusty BK, Böhme L, Bergmann B, Siegl C, Krause E et al. Imbalanced oxidative stress causes chlamydial persistence during non-productive human herpes virus co-infection. *PLoS One* 2012;7:e47427.